Ultrasound in Med. & Biol., Vol. 42, No. 6, pp. 1273–1281, 2016

Printed in the USA
0301-5629

http://dx.doi.org/10.1016/j.ultrasmedbio.2016.01.012

● *Original Contribution*

SHEAR WAVE ELASTOGRAPHY AND CERVICAL LYMPH NODES: PREDICTING MALIGNANCY

Ghobad Azizi,* James M. Keller,† Michelle L. Mayo,* Kelé Piper,‡ David Puett,§ Karly M. Earp,* and Carl D. Malchoff¶

* Wilmington Endocrinology, Wilmington, North Carolina, USA; † Wilmington Pathology Associates, Wilmington, North Carolina, USA; ‡ Children's Hospital Colorado, Research Compliance, Aurora, Colorado, USA; § Carolina Arthritis, Wilmington, North Carolina, USA; and ¶ Department of Endocrinology, University of Connecticut Health Center, Farmington, Connecticut, USA

(*Received* 6 *October* 2015; *revised* 9 *December* 2015; *in final form* 23 *January* 2016)

Abstract—This prospective study evaluates the accuracy of virtual touch imaging quantification (VTIQ), a non-invasive shear wave elastography method for measuring cervical lymph nodes (LN) stiffness in differentiating benign from malignant LN. The study evaluated 270 LN in 236 patients with both conventional B-mode ultrasound and VTIQ shear wave elastography before fine-needle aspiration biopsy (FNAB). LN stiffness was measured as shear wave velocity (SWV) in m/s. Surgical resection was advised for FNAB results that were not clearly benign. Surgical pathology confirmed 54 malignant LN. The receiver operating curve (ROC) identified a single cut-off value of 2.93 m/s as the maximum SWV for predicting a malignant cervical LN. The sensitivity and specificity were 92.59% and 75.46%, respectively. Positive predictive value (PPV) was 48.54% and negative predictive value (NPV) was 97.60%. LN stiffness measured by VTIQ–generated shear wave elastography is an independent predictor of malignancy. (E-mail: azizi@wilmingonendo.com)

Key Words: **Lymph node, Malignancy, Shear wave elastography, Fine-needle aspiration biopsy, Ultrasound.**

INTRODUCTION

Assessment of cervical lymph nodes (LN) is essential in patients with head and neck cancer because it predicts prognosis and helps in selection of treatment options (Ishii et al. 1991; Vassallo et al. 1992). B-mode ultrasound (US) imaging is widely used for pre-operative imaging of head and neck cancer (Choi et al. 2013).

Sonographic features of malignant LN include cystic content, spherical shape, central vascularity and calcification. Presence of fatty hilum suggests a benign LN (Ahuja and Ying 2003; Ying and Ahuja 2003).

Papillary thyroid carcinoma (PTC) recurs most frequently at the cervical LN, with a reported recurrence rate of up to 31% in patients. Recent studies revealed that regional LN metastasis predicts lower survival rates (Jung et al. 2015).

Address correspondence to: Ghobad Azizi, Wilmington Endocrinology, 1717 Shipyard Boulevard, Suite 220, Wilmington, NC 28403, USA. E-mail: azizi@wilmingonendo.com

Strain and shear wave elastography investigate differences in the mechanical properties of structures by applying an external force and monitoring the deformation response. Low relative displacement is linked to decreased elasticity and malignancy. This technology has been integrated into conventional US machines (Ianculescu et al. 2014; Krouskop et al. 1998).

Shear wave can quantify velocity and indirectly measure tissue stiffness. Virtual touch imaging quantification (VTIQ) is capable of creating shear wave images and subsequent tissue quantification in one display and allows for identification of regions for measurement of tissue stiffness (Benson and Fan 2012). The use of VTIQ software in the United States was approved by the FDA in June of 2013 (Bell 2013). For this manuscript we decided to use the term VTIQ instead of a generic shear wave term because of some specific features unique to this technology.

Principle of acoustic radiation force impulse elastography

VTIQ is based on the principle of acoustic radiation force impulse (ARFI) technology (Benson and Fan 2012).

Tissue is compressed using an acoustic push beam that is focused at the region of interest (ROI) to maximize the local displacement of tissue *via* the acoustic impulse. In tissue, shear waves travel at a velocity of around 1–10 m/s (Benson and Fan 2012). Using image-based localization and proprietary implementation of ARFI technology, the shear wave speed may be quantified in a precise anatomic region focused on a ROI with a pre-defined 1.5 mm size provided by the system (Sporea et al. 2011).

The VTIQ image is a color-coded display of relative shear wave velocities within the user-defined ROI superimposed onto a conventional B-mode US image. VTIQ is capable of four discrete shear wave display maps: velocity, quality, travel time and displacement (Benson and Fan 2012). The quality map is particularly important to make sure that the VTIQ image quality is appropriate. Several publications have shown that certain disease processes, including malignancy, can alter the elastic properties of tissue (Benson and Fan 2012; Rosen et al. 2008; Wellman et al. 1999).

OBJECTIVE

The purpose of this study was to assess the effectiveness of shear wave elastography with VTIQ, alone and in combination with other B-mode characteristics, in evaluating the risk of malignancy in cervical LN in the setting of a clinical endocrine practice specializing in thyroid disorders.

METHODS

We prospectively evaluated 270 LN in 231 consecutive patients from March 28, 2013 to November 12, 2014. Patients were referred for the following reasons: enlarged cervical LN (90 LN in 76 patients); thyroid nodule (TN) management where LN were found during US exam before FNAB (97 LN in 86 patients); or a history of thyroid carcinoma (TC) when enlarged LN were diagnosed during routine post-operative US exam (83 LN in 69 patients). All patients were evaluated clinically and with US by a single practitioner with more than 16 y of experience in thyroid and neck US, 8 mo experience using SWE routinely before study and whose practice is enriched in thyroid disorders. We selected LN based on US features suspicious for malignancy, and if LN did not have worrisome features, the largest LN was selected for analysis. All LN ≥15 mm in maximal dimension were sampled regardless of B-mode US features and when worrisome B-mode features were present, LN ≥5 mm were biopsied. Our reference standard was the FNAB cytology result or surgical pathology result when FNAB was unable to make a definitive diagnosis.

The *Health Insurance Portability and Accountability Act* compliant study protocol was approved by the Institutional Review Board and patients were studied both before and after the VTIQ technology was approved by the FDA. The FNAB cytopathology result or surgical result when available was considered the reference standard. The inclusion criteria were the presence of LN greater than 5 mm requiring FNAB to exclude malignancy and age 18 y or older. All patients gave written informed consent. The exclusion criteria were non-diagnostic biopsy sample who refused repeat FNAB, atypical/inconclusive FNAB result without definitive diagnosis of cancer or when patient refused recommended surgical resection to have final diagnosis.

Gender, age, and number of US determined LN were noted at the time of initial US examination.

The LN were evaluated for the following B-mode characteristics: size (length and height), cystic content, presence of a fatty hilum, calcifications and location in the neck. The axis ratio is defined as the shortest measurement divided by the longest measurement of the LN. LN were placed into two groups based on an axis ratio ≥0.5 and <0.5.

For power Doppler vascular patterns LN were divided into three groups: group 1 had no blood flow; group 2 had peripheral blood flow only; and group 3 had central blood flow (with or without peripheral vascularity). LN locations in the neck were classified as anatomic levels 2, 3, 4, 5 and 6. Figure 1 shows neck level classification based on American Joint Committee on Cancer recommendations (Som et al. 2000).

Shear wave elastography

Conventional US exam and shear wave elastography were performed with Siemens ACUSON S3000 US system (Siemens Medical Solution, Mountain View, CA, USA). The B-mode features were recorded with an 18 LHD probe. Based on the location of the LN and anatomy of the neck, we used a frequency between 8–17 MHz to assess B-mode and vascularity features. The majority of LN were assessed with a frequency between 12–15 MHz. The shear wave image was created and reproduced twice with a 9 L4 Multi-D probe. Shear wave velocity (SWV) measurement was performed using VTIQ software (Siemens Medical Solution, Mountain View, CA, USA). A small ROI box was used to measure LN tissue velocity. The stiffest area within the LN was measured twice, read 1 and 2, because the ROI box is relatively small (1.5 mm in diameter). The highest velocity was reported as the maximum SWV. Velocity mean was defined as the average of the two LN velocity measurements. The elastography exam was the last part of the US exam before FNAB.

Fine-needle aspiration biopsy procedure

Consent was obtained before performing the procedure. FNAB was performed under sterile conditions with

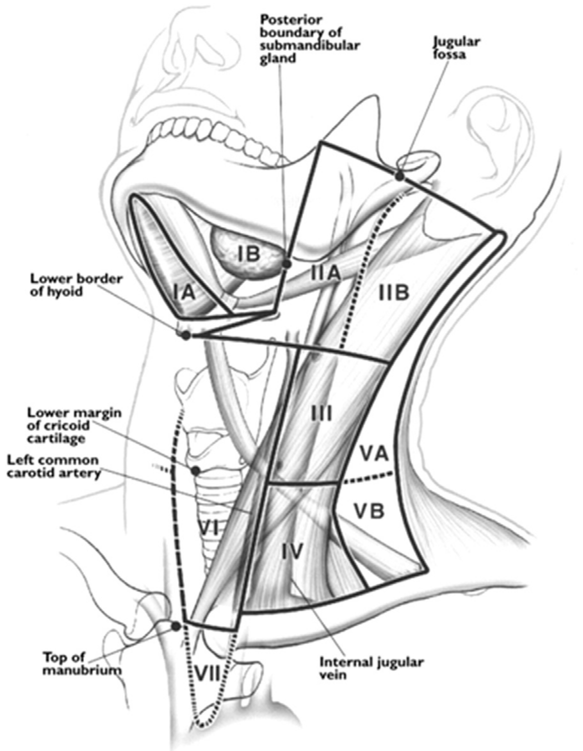

Fig. 1. This figure shows American Joint Committee on Cancer classification of cervical lymph nodes (LN). Level 1 LN are submental and sub-mandibular; level 2 LN are upper internal jugular chain nodes; level 3 LN are middle internal jugular chain nodes; level 4 LN are lower internal jugular chain nodes; level 5 LN are spinal accessory chain nodes and transverse cervical chain nodes; and level 6 LN are anterior cervical nodes (Som et al. 2000).

US guidance to confirm accurate needle placement. Two passes were made of each LN using 27-gauge needles. Cytopathology was used to determine the presence of malignancy in the LN under investigation.

Statistical analysis

The primary aim of the study is to examine SWV and B-mode US to predict risk of malignancy. In this analysis maximum SWV measurements were performed twice. We included the following B-mode US features: axis ratio, calcification, cystic content, vascularity and fatty hilum. Bivariate associations of presence or absence of cancer with key continuous variables and discrete variables were determined using Wilcoxon signed tests and chi-squared tests, respectively. Multivariate logistic regression was used to determine association of presence of cancer for each of the above variables controlling for age and gender. Receiver operating curve (ROC) was used to examine an optimum shear value that produces maximum sensitivity in predicting cancer. In addition, sensitivity, specificity and negative and positive predictive values of three levels of shear in predicting cancer is determined and each of the above predictors is examined. Statistical significance was determined at alpha of 0.05. Statistical analysis was conducted using SAS 9.3 (SAS Institute Inc., Cary, NC, USA).

RESULTS

Cytopathology and pathology

In this prospective study 277 LN in 236 patients were eligible for inclusion. Five patients with seven LN were excluded due to previously mentioned criteria. FNAB cytopathology results of the 270 LN in 231 patients enrolled in this study are discussed below.

There were a total of 216 benign LN and 54 malignant LN. For benign LN the mean size was 15.1 ± 6.2 mm, and for malignant LN the mean size was 16.3 ± 7.3 mm. The majority of malignant LN were metastatic TC. There were 39 LN with metastatic TC: one medullary TC, three follicular variant of PTC and 35 PTC. Fifteen malignant LN were related to other malignancies: six LN were positive for small cell lymphoma, five LN were metastatic squamous cell carcinoma, two LN were associated with chronic lymphocytic leukemia (CLL) and two LN contained metastatic prostate cancer in the neck. In this study, all patients with FNAB indicating metastatic TC underwent surgical resection. For the remaining 15 LN, FNAB was either diagnostic for malignancy or inconclusive. Those patients with inconclusive FNAB had surgical resection to make a final diagnosis.

See Figure 2 for examples of VTIQ display modes, including shear wave elastography image, velocity measurement and quality map. Figures 3–5 show examples of VTIQ used to diagnose malignant LN.

Bivariate analysis

The bivariate associations of benign versus malignant status of cervical LN with demographic, clinical variables and US (B-mode and elastography) characteristics are presented in Table 1.

The maximum SWV for the malignant LN was (mean ± SD) 3.96 ± 0.96 m/s, which was significantly greater than the maximum SWV of the benign LN (2.71 ± 0.65 m/s; $p < 0.0001$). The velocity mean of the two measurements of the stiffest areas of the malignant LN was significantly higher versus that of the benign LN (3.83 ± 0.9 m/s vs. 2.62 ± 0.64 m/s; $p < 0.0001$). There was no significant difference between velocity read 1 and read 2 of the stiffest area among the benign and malignant LN as shown in Table 1.

Among the demographic characteristics, patients with malignant LN were older (49.95 ± 15.74 y) than those with benign LN (45.21 ± 15 y; $p < 0.0583$).

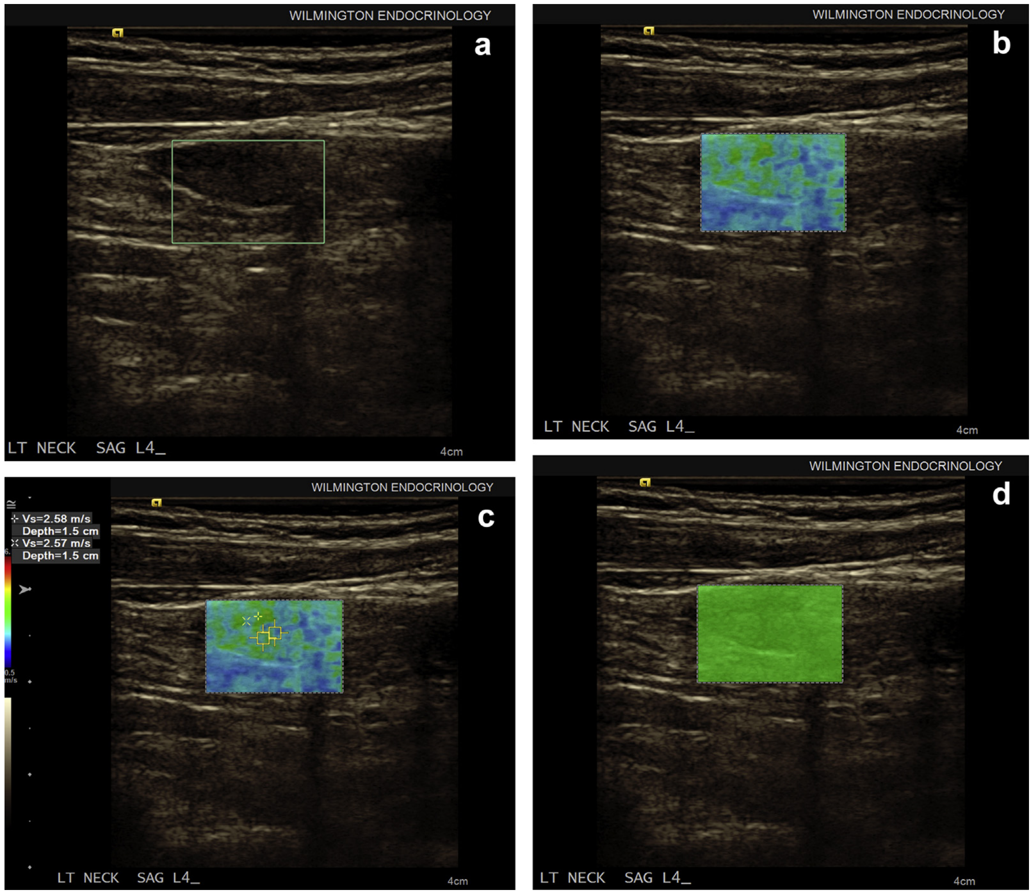

Fig. 2. (a) B-mode image of a lymph node (LN) in the left neck level 4 measuring 12.7 × 7.3 × 8.2 mm with an axis ratio >0.5. (b) Qualitative shear wave image of the LN. (c) Qualitative and quantitative shear wave image of the same LN. The maximum shear wave velocity measurements of the LN were 2.53 m/s and 2.49 m/s. (d) Quality image. The green color represents a good image quality. Fine-needle aspiration biopsy for this LN was benign.

Among the B-mode US characteristics, an axis ratio ≥0.5 was more prevalent among the malignant LN group with 29 LN (53.7%) versus 52 benign LN (24.7%; $p < 0.0001$). Other B-mode US characteristics that showed a statistical difference between malignant and benign LN groups included the presence of calcifications in malignant LN, which was higher than in the benign group (nine LN [16.67%] versus five LN [2.31%];

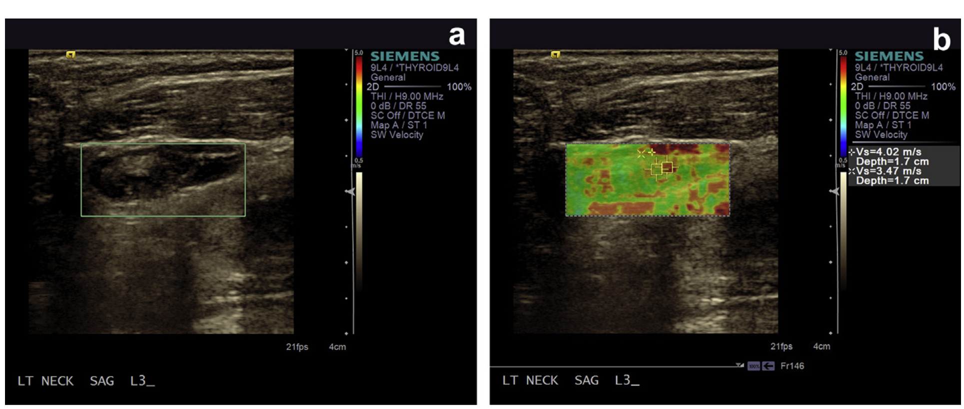

Fig. 3. (a) Lymph node (LN) in the left neck level 3 measuring 23 × 8.6 × 13 mm with an axis ratio <0.5. This LN contains fatty hilum. (b) Qualitative and quantitative shear wave image of the LN. Shear wave velocity measurements of the LN were 4.02 m/s and 3.47 m/s. Fine-needle aspiration biopsy of this LN was consistent with papillary thyroid carcinoma. Surgical pathology confirmed the diagnosis of papillary thyroid carcinoma.

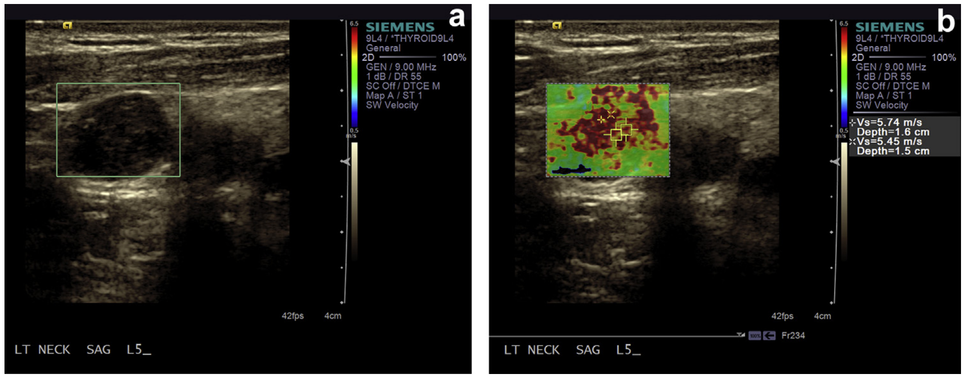

Fig. 4. (a) Lymph node (LN) in the left neck level 5 measuring 13 × 9 × 13 mm with an axis ratio >0.5. (b) Qualitative and quantitative shear wave image of the LN. Shear wave velocity measurements of the LN were 5.74 m/s and 5.45 m/s. Fine-needle aspiration biopsy of this LN was diagnostic for squamous cell carcinoma. Surgical pathology confirmed this diagnosis.

$p < 0.0001$). Among LN with cystic content 12 (22.22%) were malignant and four (1.85%) were benign ($p < 0.0001$). Fatty hilum was present more frequently in the benign group with 49 LN (22.69%) versus two malignant LN (3.7%; $p < 0.0001$). This feature was predictive of benign LN.

While lack of blood flow was predictive of benign LN, peripheral and central blood flow were predictive of malignant LN. In the bivariate analysis, based on anatomic locations, malignant LN associated with levels 2 and 4 reached statistical significance.

Receiver operating curves

The ROC (Fig. 6) was used to determine the sensitivity and specificity of the continuous variable of maximum SWV to predict malignant LN. The area under the curve for this model is 0.88 (95% confidence interval [CI]: 0.82 and 0.93). Based on the ROC curve for SWV predicting malignant LN, a single cut-off of 2.93 m/s had a sensitivity of 92.59%. The specificity, positive predictive value (PPV) and negative predictive value (NPV) were 75.46%, 48.54% and 97.6%, respectively.

Lymph nodes categorized by maximum shear wave velocity groups

We divided LN into three groups based on maximum SWV after we analyzed our statistical result: reference group 1 (0–2.6 m/s), reference group 2 (>2.6–≤3.2 m/s) and reference group 3 (>3.2 m/s). Reference group 1 had a total of 125 LN with 122 benign LN (97.60%) and 3 malignant LN (2.4%). In group 2, eight of 63 LN (12.7%) were malignant and 55 (87.3%) were benign. Group 3 had a total of 82 LN with 39 benign (47.56%) and 43 malignant (52.44%).

Multivariate analysis

Table 2 provides the age and gender adjusted logistic regression of potential predictors of malignant LN.

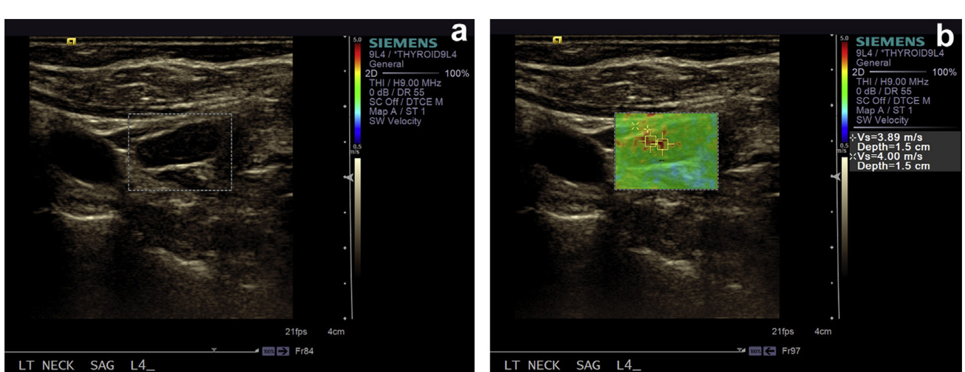

Fig. 5. (a) Lymph node (LN) in the left neck level 4 measuring 17 × 5 × 10 mm with an axis ratio >0.5. (b) Qualitative and quantitative shear wave image of the LN. Shear wave velocity measurements of the LN were 3.89 m/s and 4.00 m/s. Fine-needle aspiration biopsy, flow cytometry and subsequent surgical pathology of this LN was consistent with small cell lymphoma.

Table 1. The bivariate associations of cancer status of lymph nodes with demographic, clinical variables and ultrasound characteristics

Variable	No cancer n (%), mean (SD) (N = 216)	Cancer n (%), mean (SD) (N = 54)	*p* Value
Age	45.21 (15)	49.95 (15.74)	0.0583
Female	157 (72.69)	28 (51.85)	0.0032
LN SWV read 1	2.61 (0.63)	3.86 (0.92)	<0.0001
LN SWV read 2	2.63 (0.66)	3.81 (0.91)	<0.0001
Maximum SWV	2.71 (0.65)	3.96 (0.96)	<0.0001
Mean SWV	2.62 (0.64)	3.83 (0.9)	<0.0001
Axis ratio ≥0.5	52 (24.07)	29 (53.7)	<0.0001
Calcifications	5 (2.31)	9 (16.67)	<0.0001
Cystic LN	4 (1.85)	12 (22.22)	<0.0001
Fatty hilum	49 (22.69)	2 (3.7)	0.0014
Power Doppler group 1	201 (93.06)	33 (61.11)	<0.0001
Power Doppler group 2	8 (3.7)	7 (12.96)	0.0079
Power Doppler group 3	7 (3.24)	14 (25.93)	<0.0001
Level 2	9 (4.17)	8 (14.81)	0.0040
Level 3	62 (28.7)	13 (24.07)	0.4969
Level 4	86 (39.81)	9 (16.67)	0.0014
Level 5	25 (11.57)	10 (18.52)	0.1742
Level 6	34 (15.74)	14 (25.93)	0.0800

LN = lymph nodes; SD = standard deviation; SWV = shear wave velocity.

Calcification (OR [95% CI]: 20.433 [4.998 and 83.538]), an axis ratio ≥0.5 (OR [95% CI]: 2.855 [1.390 and 5.866]) and a cystic LN content (OR [95% CI]: 18.607 [4.720 and 73.355]) are predictive of malignant LN, while the presence of fatty hilum (OR [95% CI]: 0.186 [0.042 and 0.820]) is predictive of benign LN.

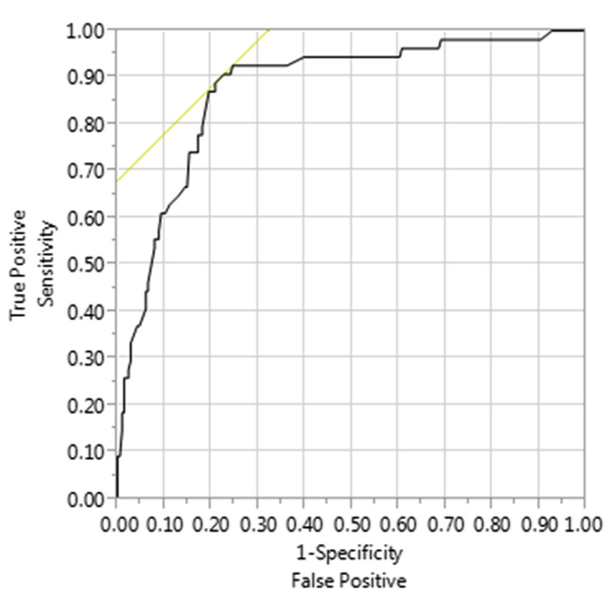

Fig. 6. A receiver operating curve shows shear wave velocity predicting malignant lymph nodes. Intersections of the *yellow line* with the curve are the points of highest sensitivity (92.59%) and specificity (75.46%).

Table 2. Multivariate predictors of cancer adjusted for age and gender

Variable	Odds ratio	95% Lower confidence interval	95% Upper confidence interval
Fatty hilum vs. reference	0.186	0.042	0.820
Calcification vs. reference	20.433	4.998	83.538
Axis ratio ≥0.5 (reference: <0.5)	2.855	1.390	5.866
Cystic vs. reference	18.607	4.720	73.355
Power Doppler			
Group 1: (reference) no blood flow			
Group 2: peripheral blood flow	5.222	1.539	17.721
Group 3: central blood flow	14.216	4.827	41.866
SWV Max			
Group 1 (reference: 0–2.6)			
Group 2: >2.6–≤3.2	5.482	1.356	22.165
Group 3: >3.2	31.431	8.937	110.537

SWV = shear wave velocity.

As indicated previously, maximum SWV was divided into three groups. Compared with the reference group (0–2.6 m/s), the SWV group 2 (>2.6–≤3.2; OR [95% CI]: 5.482 [1.356 and 22.165]) and group 3 (SWV >3.2) (OR [95% CI]: 31.431 [8.937 and 110.537]) were predictive of malignant LN. The odds of predicting malignancy compared to the reference group progressively increased with higher SWV.

Power Doppler (PD) groups were also included in this analysis. When using the PD group 1 as the reference group, PD group 2 (OR [95% CI]: 5.222 [1.539 and 17.721]) and PD group 3 (OR [95% CI]: 14.216 [4.827 and 41.866]) were predictive of malignancy.

Neck levels that were statistically significant in bivariate (levels 2 and 4) did not quite reach statistical significance in multivariate analysis as a predictor of malignancy.

Sensitivity and specificity

In single cut-off analysis for predicting malignancy, LN with maximum SWV ≥2.93 m/s had the best sensitivity of 92.59%. The specificity, PPV and NPV were 75.46%, 48.54% and 97.6%, respectively. For the highest SWV group (>3.2 m/s) the prevalence of malignant LN was 52.44% with a sensitivity, specificity, PPV and NPV of 79.63%, 81.94%, 52.44% and 94.15%, respectively. Table 3 shows the sensitivity, specificity, PPV and NPV for each respective SWV group, B-mode characteristics and power Doppler.

Maximum shear wave velocity of lymph nodes in sub-group

In this sub-group analysis, we divided patients based on their reason for referral. In the group of patients who were referred for enlarged LN, there were 19 malignant LN with a mean SWV of 4.35 ± 1.22 m/s and 71 benign

Table 3. Sensitivity, specificity and positive and negative predictive values for predicting malignant lymph nodes for various cut-offs of maximum shear wave velocity and B-mode characteristics

Value of maximum velocity (m/s) predicting malignant LN	Sensitivity	Specificity	PPV	NPV
≥2.93 vs. <2.93 (reference <2.93)	50/54 (92.59%)	163/216 (75.46%)	50/103 (48.54%)	163/167 (97.60%)
>3.2 vs. ≤3.2 (reference ≤3.2)	43/54 (79.63%)	177/216 (81.94%)	43/82 (52.44%)	177/188 (94.15%)
B-Mode characteristics predicting malignant LN				
Axis ratio ≥0.5 vs. <0.5	29/54 (53.70%)	164/216 (75.93%)	29/81 (35.80%)	164/189 (86.77%)
Calcification Yes vs. no	9/54 (16.67%)	211/216 (97.69%)	9/14 (64.29%)	211/256 (82.42%)
Cystic content Yes vs. no	12/54 (22.22%)	212/216 (98.15%)	12/16 (75%)	212/254 (83.46%)
Power Doppler Group 3 vs. group 1	14/47 (29.79%)	201/208 (96.63%)	14/21 (66.67%)	201/234 (85.90%)
Fatty hilum predicting malignant LN	2/54 (3.70%)	167/216 (77.31%)	2/51 (3.92%)	167/219 (76.26%)
Fatty hilum predicting benign LN	52/54 (96.3%)	49/216 (22.69%)	49/51 (96.08%)	52/219 (23.74%)

LN = lymph nodes; NPV = negative predictive value; PPV = positive predictive value.

LN with a mean SWV of 2.79 ± 0.64 m/s. Among patients referred for TN where LN was found during routine exam, there were 17 malignant LN with a mean SWV of 3.69 ± 0.48 m/s and 80 benign LN with a mean SWV of 2.56 ± 0.51 m/s. In the last group of patients with a history of TC who had routine post-operative neck US, there were 18 malignant LN with a mean SWV of 3.81 ± 0.84 m/s and 65 benign LN with a mean SWV of 2.79 ± 0.77 m/s. SWV for all benign LN was very similar.

Maximum shear wave velocity of malignant lymph nodes groups

In an additional sub-group analysis of the 54 malignant LN, there were 39 LN with metastatic TC. The mean SWV ± SD for this group was 3.88 ± 0.85 m/s. Among LN with small cell lymphoma and CLL, the mean SWV was 3.47 ± 0.90 m/s. LN with metastatic squamous cell carcinoma had the highest mean SWV of 5.40 ± 0.81 m/s. Finally, the two LN with prostate cancer had a mean SWV of 4.65 ± 0.15 m/s.

DISCUSSION

The purpose of this prospective study was to evaluate the performance of VTIQ generated SWV for predicting the risk of malignancy in cervical LN in patients presenting to a clinical thyroid practice. Tissue stiffness was assessed by creating shear wave images and subsequent tissue quantification in one display. The tissue velocity is measured in m/s and directly correlates with tissue stiffness.

Based on the ROC curve, the best single cut-off maximum SWV for predicting malignant LN was 2.93 m/s with a sensitivity of 92.59%. The specificity, PPV and NPV were 75.46%, 48.54% and 97.6%, respectively. Compared with B-mode US features for predicting malignancy, maximum SWV has a higher sensitivity and a higher NPV that are likely to be clinically useful.

In a second analysis, LN were divided into three predetermined groups based on maximum SWV. In group 3, with the highest SWV >3.2 m/s (OR [95% CI]: 31.431 [8.937 and 110.537]), 52.44% of LN (43 of 84 LN) were malignant. When we compared these two cut-offs, the ROC curve (2.93 m/s) had a better sensitivity and NPV, while the >3.2 m/s cut-off had a better specificity and PPV. In group 1 (SWV 0–2.6 m/s), 2.40% of LN (3 of 125 LN) were malignant and 97.6% were benign. Both the multi cut-off and single cut-off were effective in distinguishing benign from malignant LN. A larger study is required to validate or establish a single or multi cut-off SWV to determine the risk for malignancy in cervical LN. In a pilot study of 55 cervical LN performed with Supersonic US, Bhatia et al. (2012) demonstrated that SWV in malignant LN was higher than in benign LN.

B-mode US characteristics of benign and malignant LN observed in this study are similar to those described by others. B-mode features suggestive of malignancy include an LN axis ratio ≥0.5, cystic content, calcification and vascularity (Ahuja and Ying 2002, 2003; Bhatia et al. 2011; Tohnosu et al. 1989; Vassallo et al. 1993; Ying and Ahuja 2003; Ying et al. 1996).

In our study, B-mode US LN characteristics of cystic content and calcifications predicted malignant LN with a high specificity of 98.1% and 97.69%, respectively. However, these features are not common, so the sensitivity was low. The sensitivity of predicting cancer for cystic content and calcification was 22.22% and 16.67%, respectively. In this study, calcification in malignant LN was associated only with metastatic PTC and was not present with other malignant LN. Other studies reported this finding as well (Som 1987, 1992).

Since worrisome B-mode features for LN, like calcification and cystic content, are uncommon, an axis ratio ≥0.5 is presently the most common B-mode feature that distinguishes benign and malignant LN. We had 81 LN with an axis ratio ≥0.5 (OR [95% CI]: 2.855 [1.390 and 5.866]); 52 were benign and 29 were malignant.

Lack of vascularity is predictive of benign LN ($p < 0.0001$). Both peripheral and central vascularity are predictive of malignancy, with the latter being a stronger predictor. Other publications reported the association of peripheral and central vascularity with malignant LN (Ahuja et al. 1997; Dragoni et al. 1999; Na et al. 1997; Steinkamp et al. 1998).

The presence of fatty hilum is, in general, predictive of benign LN (Rubaltelli et al. 1990; Solbiati et al. 1992). In this study, 51 LN contained fatty hilum. Among this group, two LN were malignant and 49 were benign. This B-mode characteristic has a high sensitivity, but a low specificity and NPV for predicting benign cervical LN.

In this study, location of an LN in the neck based on anatomic classification level (2, 3, 4, 5 or 6) was not a predictor for malignancy in the multivariate analysis.

The SWV for benign LN was very similar regardless of their reason for referral. SWV for malignant LN was higher when patients were referred for enlarged LN, but did not reach statistical significance.

In this study, LN with squamous cell carcinoma had the highest maximum SWV followed by prostate cancer, TC and small cell lymphoma and CLL. A larger study may be needed to examine the difference in SWV among metastatic LN. Thirty-nine of 54 malignant LN were metastatic TC. Twenty-seven of these malignant LN were diagnosed before thyroid surgery while the remaining 12 were diagnosed during routine post-operative monitoring. This data demonstrates that this technology can be helpful both pre- and post-operative when combined with B-mode.

We did not analyze the performance of VTIQ with thyroglobulin washout. The purpose of this study was to compare the performance of non-invasive LN evaluations. In addition, thyroglobulin washout is useful only when evaluating for TC and would have missed all remaining malignant LN.

The strengths of this study include the prospective design and large number of LN evaluated.

Limitations of virtual touch imaging quantification

Several factors may alter the SWV or make measurement difficult. LN deeper than 4 cm are difficult to evaluate, as are LN in patients with thick or short necks. Close posterior proximity to large vasculature can limit evaluation due to motion artifact. Evaluation of LN near the trachea, the posterior aspect of thyroid gland and at level 6 can be challenging. LN with a large or thick hilum can show higher SWV as well. A larger multicenter trial may be needed to validate our findings.

Finally, since not all enlarged cervical LN were sampled, there may have been a selection bias. This is a limitation of almost all FNAB studies.

CONCLUSION

In summary, in a single cut-off analysis, the best SWV predicting malignancy in cervical LN is 2.93 m/s with a sensitivity of 92.59%. The specificity, PPV and NPV were 75.46%, 48.54% and 97.6%, respectively.

In a multi cut-off analysis, the rate of malignant LN in the group with highest SWV (>3.2 m/s) was 52.44%. The lowest SWV group (0–2.6 m/s) had a rate of 2.40% for malignant LN and 97.60% rate for benign LN.

We conclude that LN stiffness measured by VTIQ–generated quantitative shear wave elastography is an independent predictor of malignant LN. Our data suggest that application of shear wave elastography may decrease the number of FNAB for low risk LN and improve the ability to select LN with high probability for malignancy.

Acknowledgments—For performing the statistical analysis and for expert statistical advice, we acknowledge Maggie M. Kuchibhatla, PhD (Duke University, Durham, NC). We would like to thank John Benson of Siemens Medical Ultrasound Division for technical support and providing VTIQ software before FDA clearance; and the Wilmington Endocrinology staff, especially Brandy Lundberg and Caroline Driscoll, for their efforts and dedication to this prospective study.

REFERENCES

Ahuja A, Ying M. An overview of neck node sonography. Invest Radiol 2002;37:333–342.

Ahuja A, Ying M. Sonography of neck lymph nodes. Part II: Abnormal lymph nodes. Clin Radiol 2003;58:359–366.

Ahuja A, Ying M, King W, Metreweli C. A practical approach to ultrasound of cervical lymph nodes. J Laryngol Otol 1997;111:245–256.

Bell J. Siemens Announces FDA Clearance of Virtual Touch Elastography Imaging. Available at: http://usa.healthcare.siemens.com/press/pressreleases/healthcare-news-2013-06-24-1; 2013. Accessed February 15, 2016.

Benson J, Fan L. Tissue Strain Analytics – A Complete Ultrasound Solution for Elastography. Available at: http://sonoworld.com/Common/DownloadFile.aspx?ModuleDocumentsId=66; 2012. Accessed February 15, 2016.

Bhatia K, Tong CS, Cho CC, Yuen EH, Lee J, Ahuja AT. Reliability of shear wave ultrasound elastography for neck lesions identified in routine clinical practice. Ultraschall Med 2012;33:463–468.

Bhatia KS, Rasalkar DP, Lee YP, Wong KT, King AD, Yuen HY, Ahuja AT. Cystic change in thyroid nodules: A confounding factor for real-time qualitative thyroid ultrasound elastography. Clin Radiol 2011;66:799–807.

Choi YJ, Lee JH, Lim HK, Kim SY, Han MW, Cho KJ, Baek JH. Quantitative shear wave elastography in the evaluation of metastatic cervical lymph nodes. Ultrasound Med Biol 2013;39:935–940.

Dragoni F, Cartoni C, Pescarmona E, Chiarotti F, Puopolo M, Orsi E, Pignoloni P, De Gregoris C, Mandelli F. The role of high resolution pulsed and color Doppler ultrasound in the differential diagnosis of benign and malignant lymphadenopathy: Results of multivariate analysis. Cancer 1999;85:2485–2490.

Ianculescu V, Ciolovan LM, Dunant A, Vielh P, Mazouni C, Delaloge S, Dromain C, Blidaru A, Balleyguier C. Added value of virtual touch IQ shear wave elastography in the ultrasound assessment of breast lesions. Eur J Radiol 2014;83:773–777.

Ishii J, Amagasa T, Tachibana T, Shinozuka K, Shioda S. US and CT evaluation of cervical lymph node metastasis from oral cancer. J Craniomaxillofac Surg 1991;19:123–127.

Jung WS, Kim JA, Son EJ, Youk JH, Park CS. Shear wave elastography in evaluation of cervical lymph node metastasis of papillary thyroid carcinoma: Elasticity index as a prognostic implication. Ann Surg Oncol 2015;22:111–116.

Krouskop TA, Wheeler TM, Kallel F, Garra BS, Hall T. Elastic moduli of breast and prostate tissues under compression. Ultrason Imaging 1998;20:260–274.

Na DG, Lim HK, Byun HS, Kim HD, Ko YH, Baek JH. Differential diagnosis of cervical lymphadenopathy: Usefulness of color Doppler sonography. AJR Am J Roentgenol 1997;168:1311–1316.

Rosen J, Brown JD, De S, Sinanan M, Hannaford B. Biomechanical properties of abdominal organs *in vivo* and postmortem under compression loads. J Biomech Eng 2008;130:021020.

Rubaltelli L, Proto E, Salmaso R, Bortoletto P, Candiani F, Cagol P. Sonography of abnormal lymph nodes *in vitro*: Correlation of sonographic and histologic findings. AJR Am J Roentgenol 1990;155: 1241–1244.

Solbiati L, Cioffi V, Ballarati E. Ultrasonography of the neck. Radiol Clin North Am 1992;30:941–954.

Som PM. Lymph nodes of the neck. Radiology 1987;165:593–600.

Som PM. Detection of metastasis in cervical lymph nodes: CT and MR criteria and differential diagnosis. AJR Am J Roentgenol 1992;158: 961–969.

Som PM, Curtin HD, Mancuso AA. Imaging-based nodal classification for evaluation of neck metastatic adenopathy. AJR Am J Roentgenol 2000;174:837–844.

Sporea I, Vlad M, Bota S, Sirli RL, Popescu A, Danila M, Sendroiu M, Zosin I. Thyroid stiffness assessment by acoustic radiation force impulse elastography (ARFI). Ultraschall Med 2011;32:281–285.

Steinkamp HJ, Mueffelmann M, Böck JC, Thiel T, Kenzel P, Felix R. Differential diagnosis of lymph node lesions: A semiquantitative approach with colour Doppler ultrasound. Br J Radiol 1998;71: 828–833.

Tohnosu N, Onoda S, Isono K. Ultrasonographic evaluation of cervical lymph node metastases in esophageal cancer with special reference to the relationship between the short to long axis ratio (S/L) and the cancer content. J Clin Ultrasound 1989;17:101–106.

Vassallo P, Edel G, Roos N, Naguib A, Peters PE. *In-vitro* high-resolution ultrasonography of benign and malignant lymph nodes. A sonographic-pathologic correlation. Invest Radiol 1993;28:698–705.

Vassallo P, Wernecke K, Roos N, Peters PE. Differentiation of benign from malignant superficial lymphadenopathy: The role of high-resolution US. Radiology 1992;183:215–220.

Wellman PS, Howe RD, Dalton E, Kern KA. Breast tissue stiffness in compression is correlated to histological diagnosis. Technical Report. Harvard BioRobotics Laboratory 1999;1–15.

Ying M, Ahuja A. Sonography of neck lymph nodes. Part I: Normal lymph nodes. Clin Radiol 2003;58:351–358.

Ying M, Ahuja A, Brook F, Brown B, Metreweli C. Sonographic appearance and distribution of normal cervical lymph nodes in a Chinese population. J Ultrasound Med 1996;15:431–436.